



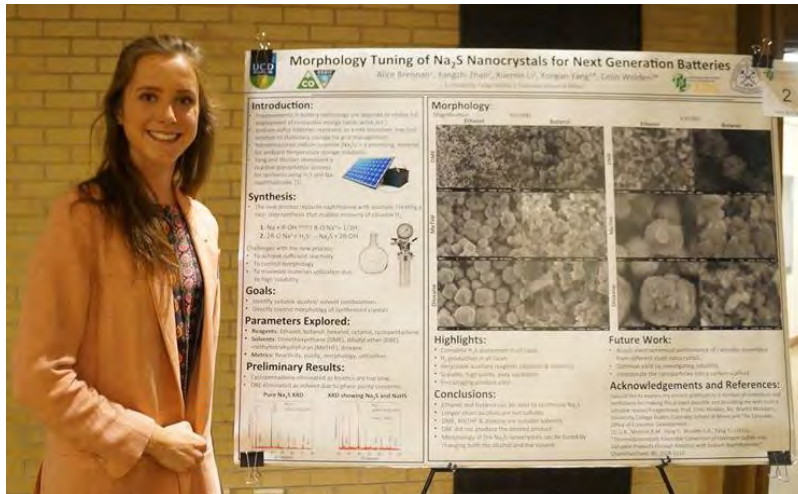
**UCD School of Chemical & Bioprocess Engineering**

**Pat McAdam Scholarship in  
Chemical & Bioprocess Engineering 2016**

**Report**

**Author:  
Alice Brennan**

## Pat McAdam Scholarship in Chemical & Bioprocess Engineering 2016



**ALICE BRENNAN**  
UCD Pat McAdam Scholar in  
Chemical & Bioprocess  
Engineering, pictured at the  
REMSEC REU Poster Session,  
Colorado School of Mines  
July 2016

### PAT McADAM SCHOLARSHIP IN CHEMICAL & BIOPROCESS ENGINEERING: PERSONAL REFLECTIONS

As a result of the exceedingly generous Pat McAdam Scholarship I had the opportunity to spend 10 weeks conducting research at the Colorado School of Mines during Summer 2016. This genuinely was the best Summer of my life to date. I lived in college dorms with approximately 30 American undergraduate science and engineering students who were also carrying out research for the Summer. In our free time we hiked many of Colorado's majestic mountains, white water rafted and sampled some of Colorado's world famous craft beers! Despite the experience only lasting 10 weeks I really made friends of a lifetime. Already I have reunited with some of them in Boulder, Santa Barbara, New York, Washington DC and back in Ireland.

Of course, I also actively participated in a research group, working under the supervision of Prof. Colin Wolden. This research, documented in the attached Technical Report, was focused on next-generation batteries. My role involved synthesising sodium sulphide nano particles for cathodes. More specifically I was investigating the impact of different reaction parameters on the morphology of the nano particles. Although I was very new to the field of battery research I was delighted by the contribution I was able to make to the project. The research group were extremely welcoming and really encouraged me to get involved in discussions and to express my opinion on how we should progress. At the end of the Summer I presented my work at a poster exhibition and wrote a report. Since then, the research has been published and I am delighted to be a co- author on the paper.[Li et al., 2017]

### REFERENCE

Li, X., Zhao, Y., **Brennan, A.**, McCeig, M., Wolden, C.A. & Yang, Y. 2017, "Reactive Precipitation of Anhydrous Alkali Sulfide Nanocrystals with Concomitant Abatement of Hydrogen Sulfide and Cogeneration of Hydrogen", *ChemSusChem*, 10 (14): 2904-2913.

## Synthesis and Morphology Tuning of Sodium Sulfide Nanocrystals for Next Generation Batteries

Alice Brennan,<sup>[a]</sup> Yangzhi Zhao,<sup>[b]</sup> Xuemin Li,<sup>[b]</sup> Yongan Yang\*<sup>[b]</sup> and Colin Wolden\*<sup>[c]</sup>

[a] School of Chemical & Bioprocess Engineering, University College Dublin

[b] Department of Chemistry and Geochemistry, Colorado School of Mines

[c] Department of Chemical and Biological Engineering, Colorado School of Mines

### Abstract:

Sodium sulfide (Na<sub>2</sub>S) nanoparticles have the potential to be very exciting new cathode materials for stationary energy storage devices. These devices would be attractive for grid- scale applications due to their low cost, abundance, reasonable power and energy densities and temperature stability. A previous paper developed a method for Na<sub>2</sub>S nanoparticle synthesis, (Li, *et al.*, 2015) where sodium naphthalenide (Na-NAP) in dimethoxyethane (DME) is used to capture H<sub>2</sub>S to produce anhydrous Na<sub>2</sub>S nanocrystals and 1,4-dihydronaphthalene. This process is extremely attractive as it provides a mechanism for complete H<sub>2</sub>S abatement while yielding the value- added nanocrystals via a thermodynamically favoured process. Here we build on this work. Specifically, the naphthalene and DME in the original reaction are replaced by a variety of different alcohols and solvents. This allows for the manipulation of the morphology of the Na<sub>2</sub>S, which will be of great importance when these nanocrystals are incorporated into battery cathodes. Furthermore, this reaction results in the production of H<sub>2</sub> instead of 1,4- dihydronaphthalene and the alcohol and solvent is directly regenerated and can be reused. This adds further to the green chemistry nature of the reaction while making it even more economically attractive for industrial scale applications.

### Introduction:

Extensive research has been conducted into cathodes incorporating lithium- sulfide nanoparticles. This has yielded batteries with superior (dis)charge capacity, cycling stability, output voltage, and voltage efficiency. In contrast, little research has been conducted into the analogous sodium- based battery systems. The higher theoretical- specific energy of lithium systems, (2,500 W h kg<sup>-1</sup>) as compared to sodium systems (1,274 W h kg<sup>-1</sup>) indicates that lithium based systems will always be preferable for applications in transportation. However, in grid- related applications, scale and cost are as important as performance. This suggests that cheap and abundant sodium may be a more economically attractive option.

High temperature sodium- sulfur (Na-S) batteries operated at >300°C with molten electrodes and a solid  $\beta$  – alumina electrolyte have already been commercialised for stationary- energy storage systems, confirming that this cell chemistry can meet the scale and cost requirements for feasibility in grid-scale applications. Since the 1980s more than 20 Na- S battery demonstrations have been installed in Japan, including two 6-megawatt plants at TEPCO stations. Each plant provides up to 48 megawatt-hours of energy storage for daily load leveling applications. This reduces the amount of generation needed during hours of peak usage. In 2006, a 1,000-kW Na-S battery system was delivered to American Electric Power by NGK Insulators, Ltd. This was the first commercial- scale application of the Na- S battery system outside Japan. As of 2011 there were 200 Na- S installations for grid applications worldwide, accounting for 315MW of discharge power capacity.

These batteries require temperatures in the region of 300°C in order to use liquid- state sulphur and sulphide positive electrodes and sodium negative electrodes, and to enhance the conductivity of the  $\beta''$ - alumina solid electrolyte. This results in a fraction of the available energy having to be used to maintain this temperature, lowering the overall efficiency (87%). Furthermore, phase limitation results in the final discharge product of high temperature Na- S batteries being Na<sub>2</sub>S<sub>x</sub> (x $\geq$ 3), (Sudworth & Tilley, 1985). A higher capacity battery could be realised if the final discharge product was Na<sub>2</sub>S.

Ambient temperature Na- S batteries are in the early stage of development and have yet to be commercialised. Only a few publications on the room temperature cell chemistry of Na- S batteries are currently available, with the majority having appeared in the last four years, (figure 1). However, a sodium- sulfur battery with a final discharge product of Na<sub>2</sub>S has been designed. This battery can cycle with just 0.31% capacity decay per cycle, 600mAhg<sup>-1</sup> reversible capacity and nearly 100% Coulombic efficiency, (Wei, *et al.*, 2016).

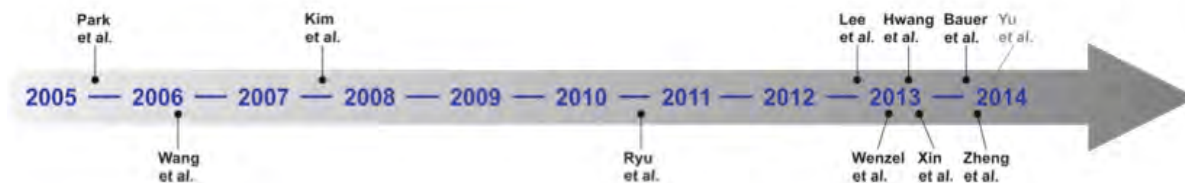


**Figure 1:** Literature timeline of research papers on room temperature Na/S<sub>8</sub> batteries (ranked after date of acceptance). Experimental studies: all journal publications in which full discharge-charge capacity profiles were shown for at least one complete cycle. Figure taken from Adelhelm *et al.*, 2015.

There are a number of challenges associated with ambient-temperature Na-S batteries that have hindered their development. Firstly the larger difference in size between Na atoms and ions than that between Li atoms and ions is believed to make sodium even more prone to form unstable electrodeposits and dendrites on the sodium metal anode, (Adelhelm *et al.*, 2015). These can grow and penetrate the separator, potentially causing short-circuit, thermal runaway, and even severe fire. Secondly, it is difficult to engineer the sulfur cathode to provide sufficient void space to accommodate the 170% volume expansion of the cathode on cell discharge, (Adelhelm *et al.*, 2015). An alternative approach that avoids these problems is to use Na<sub>2</sub>S as the cathode. This potentially removes the need to employ a sodium metal anode. Furthermore, Na<sub>2</sub>S is fully sodiated and thus is the state in which the cathode will occupy its largest volume. Therefore, there is no need to engineer a preset void space around the Na<sub>2</sub>S particles for accommodating the detrimental volume fluctuations that occur during the charge/discharge cycles. Moreover, Na<sub>2</sub>S allows batteries to be assembled in the “discharged” state, a safer and more cost-effective process. Finally, scientists have shown that the issues of poor electronic and ionic conductivity for Li<sub>2</sub>S could be overcome by using nanoparticles, (Wu, *et al.*, 2014). It is reasonable to suggest that Na<sub>2</sub>S nanoparticles would exhibit similar characteristics.

A previous paper developed a method for Na<sub>2</sub>S nanoparticle synthesis, (Li, *et al.*, 2015) where sodium naphthalenide (Na-NAP) in dimethoxyethane (DME) is used to capture H<sub>2</sub>S to produce anhydrous Na<sub>2</sub>S nanocrystals and 1,4-dihydronaphthalene. One extremely attractive feature of this process is that it provides a mechanism for complete H<sub>2</sub>S abatement while yielding the value-added nanocrystals via a thermodynamically favoured process. H<sub>2</sub>S is an extremely hazardous chemical waste that is generated at large scale in many industries. Up until

now, its abatement has been an energy-intensive and cost-ineffective liability due to the thermodynamic limitations of the selected approaches and low value of the final products, sulfur and water.

Here we build on this work in order to facilitate the tuning of the morphology of the nanoparticles. Specifically, the naphthalene and DME in the original reaction are replaced by a variety of different alcohols and solvents resulting in the synthesis of Na<sub>2</sub>S nanocrystals with very different morphologies. The alcohols investigated are ethanol, butanol, hexanol and octanol. The solvents investigated are dimethoxyethane (DME), dibutyl ether (DBE), methyl tetrahydrofuran (MeTHF) and dioxane.

Furthermore, this modification of the original reaction allows for regeneration of the original alcohols and solvents and direct production of H<sub>2</sub> gas. This adds further to the green chemistry nature of this reaction while making it even more economically attractive for industrial scale applications.

### Experiment and Results

The first step involves reacting 4mmol of sodium with 32mmol of the desired alcohol. When the sodium is completely dissolved, 40ml of solvent is added. This solution is charged to a Parr reactor and connected to a H<sub>2</sub>S stream (10% in argon) and a pure argon stream, (figure 2). Initially the H<sub>2</sub>S/ Ar mixture flows through a bypass line at ambient temperature and pressure, (40sccm of H<sub>2</sub>S and 40sccm of argon). Subsequently, the H<sub>2</sub>S stream is turned off and the argon is redirected into the reactor in order to flush the sparger. Afterwards, the H<sub>2</sub>S stream is reopened and the reaction between the H<sub>2</sub>S and the sodium alkoxide commences. 11.2 minutes was determined to provide the optimum molar ratio between the sodium alkoxide and the H<sub>2</sub>S consumed.

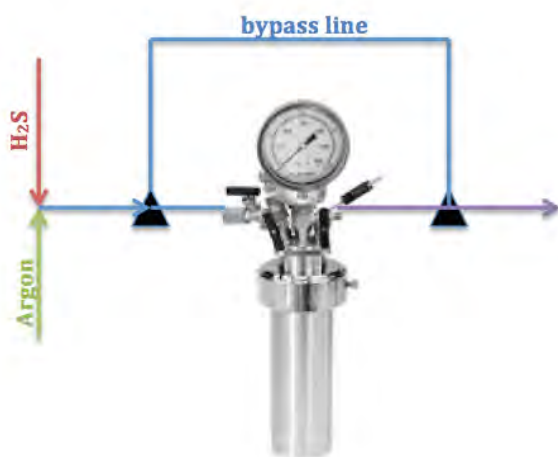


**Figure 2:** Schematic depicting the Parr reactor and associated inlet, bypass and outlet lines

Subsequently, in the glove box, centrifugation is employed to separate the solid product from the reaction solution. The collected solid powder is washed with solvent a few times before being dried for further analysis.

Figure 3 plots the time evolution of the signal intensity for argon and H<sub>2</sub>S recorded by the online quadrupole mass spectrometer (QMS), for a typical reaction. Initially, the H<sub>2</sub>S/Ar mixture flowed through a bypass line to establish a baseline reading. When the bypass was closed at t = 280 s, both argon and H<sub>2</sub>S fall exponentially with a time constant characteristic of the gas dynamics of the sampling apparatus. At t = 350 s, the inlet and outlet valves of the reactor were opened simultaneously, and the argon signal immediately increases. In stark contrast, the H<sub>2</sub>S signal continues to exponentially decay, eventually dropping below the instrument's detection limit. This indicates that the H<sub>2</sub>S supplied has been consumed at least 99.9%. Thus, the consumption of H<sub>2</sub>S through this reaction mechanism is demonstrated to be spontaneous, complete, and nearly instantaneous, as previously observed for the Na-NAP system, (Li, 2015).

The first step in the process was to determine what alcohols were compatible with the reaction. Ethanol (figure 4a) and butanol (figure 4b) successfully yielded pure Na<sub>2</sub>S nanocrystals using DME as a solvent. In contrast, the use of both hexanol (figure 4c) and octanol (figure 4d) yielded a mixture of both Na<sub>2</sub>S

and NaHS. This indicates that long chain alcohols are not suitable for use in this reaction.

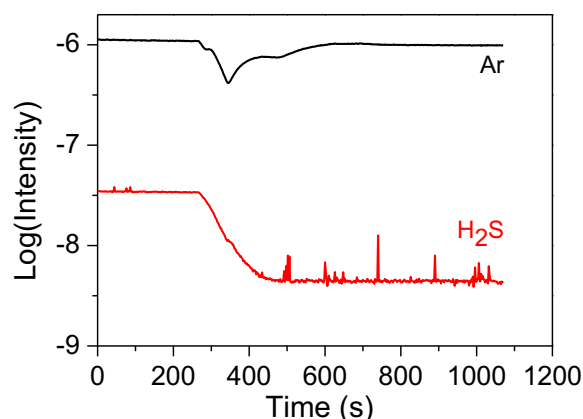


**Figure 3:** Time evolution of QMS to monitor the concentrations of key species in the gas phase: argon (black), H<sub>2</sub>S (red).

The various experiments conducted and the results obtained are detailed in Table 1.

Reagent	Solvent	XRD	Yield
Ethanol	DME	Na <sub>2</sub> S	64%
Butanol	DME	Na <sub>2</sub> S	53%
Hexanol	DME	Na <sub>2</sub> S+NaHS	
Octanol	DME	Na <sub>2</sub> S+NaHS	
Ethanol	DBE	Na <sub>2</sub> S+NaHS	
Butanol	DBE	Na <sub>2</sub> S+NaHS	
Ethanol	Methyl-THF	Na <sub>2</sub> S	50%
Butanol	Methyl-THF	Na <sub>2</sub> S	68%
Ethanol	Dioxane	Na <sub>2</sub> S	39%
Butanol	Dioxane	Na <sub>2</sub> S	71%

**Table 1:** Experimental conditions investigated and results obtained

After this, it was desired to investigate the impact of different solvents on the morphology of the nanocrystals. Interestingly, it was found that DBE resulted primarily in the synthesis of NaHS with only small quantities of Na<sub>2</sub>S (figures 4e & f). DME (figures 4a & b), methyl- THF (figures 4g & h) and dioxane (figures 4i & j) have all been identified as suitable solvents for the synthesis of pure Na<sub>2</sub>S with both ethanol and butanol. The percentage yield was also calculated for each experiment, (table 1).

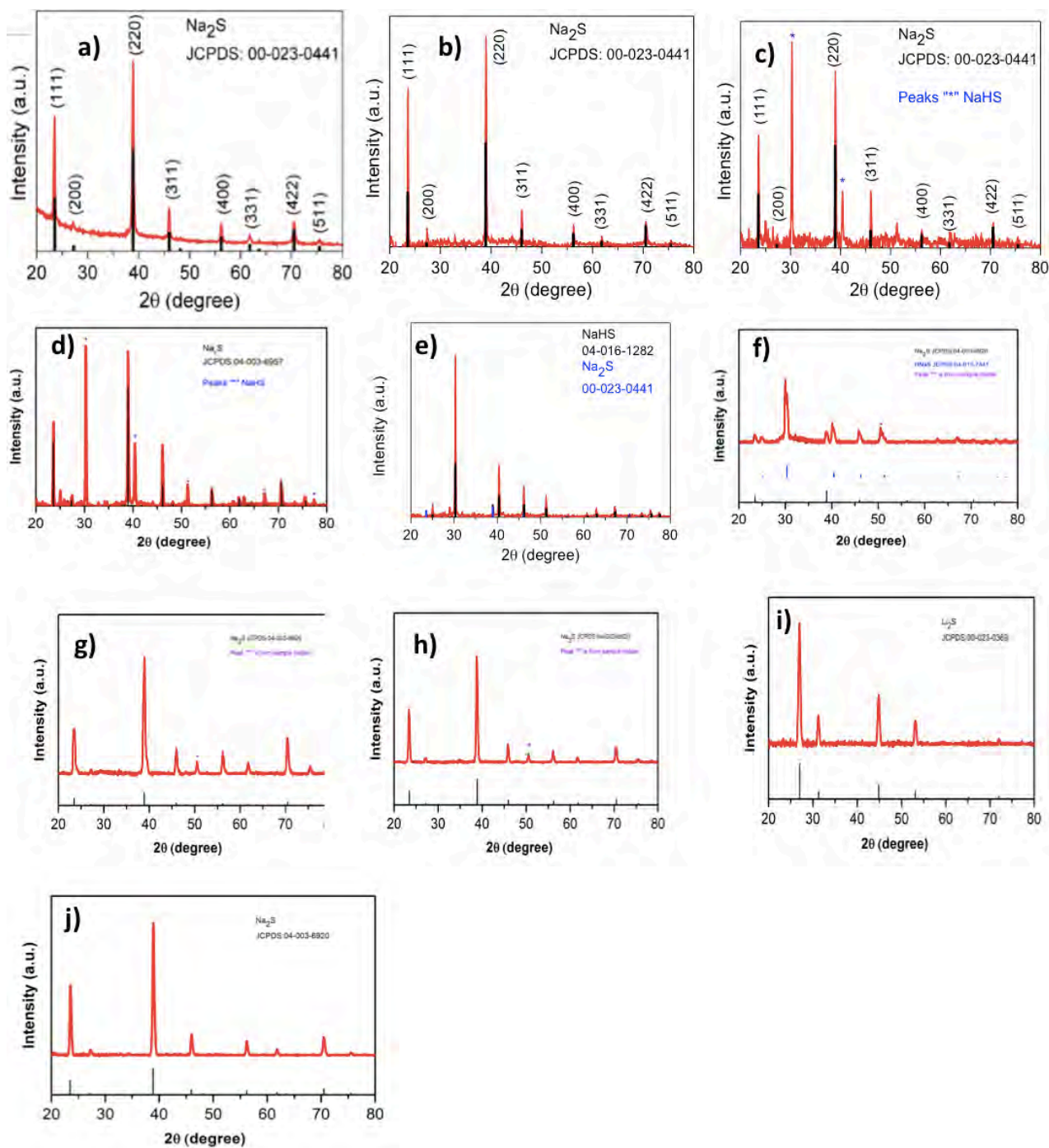


**Figure 4:** XRD from reaction of  $H_2S$  with **a)** sodium ethoxide in DME **b)** sodium butoxide in DME **c)** sodium hexoxide in DME **d)** sodium octoxide in DME **e)** sodium ethoxide in DBE **f)** sodium butoxide in DBE **g)** sodium ethoxide in methyl- THF **h)** sodium butoxide in methyl- THF **i)** sodium ethoxide in dioxane and **j)** sodium butoxide in dioxane

Scanning electron microscope images were used to determine the morphology of the  $Na_2S$  nanocrystals produced using the various alcohols and solvents. Figures 5 and 6 indicate that both ethanol and butanol in DME result in the formation of nanocubes. However, the nanocubes from the ethanol system appear to have a shorter edge

length, ( $\sim 100nm$  versus  $\sim 200nm$ ) Furthermore, the butanol in DME results in more clumping of the particles into secondary structures than ethanol in DME. These secondary structures appear to be spherical in shape with a radius of approximately  $0.5\mu m$ .

Once again, secondary clumping is evident when ethanol is used with methyl THF as a solvent, (figures 7 & 8). However, in this case, distinct nanocubes can not be observed. Instead, plate like structures seem to clump into spheres of various sizes. The radii of these spheres appear to range from  $0.2\ \mu\text{m}$  to  $1\ \mu\text{m}$ . Plate like structures are also synthesised when butanol is used with methyl THF. However, there is considerably less secondary clumping.

Ethanol and butanol in dioxane result in  $\text{Na}_2\text{S}$  crystals with very different morphologies. Figure 9 shows the ball shaped clusters formed when ethanol is employed as the alcohol. These clusters are relatively uniform in size (radii in the region of  $0.5\sim 1\ \mu\text{m}$ ) and are composed of  $100\text{nm}$  particles. In contrast, a coral shaped structure is formed with butanol, (figure 10). This is composed of numerous particles with edge lengths of approximately  $200\text{nm}$ .

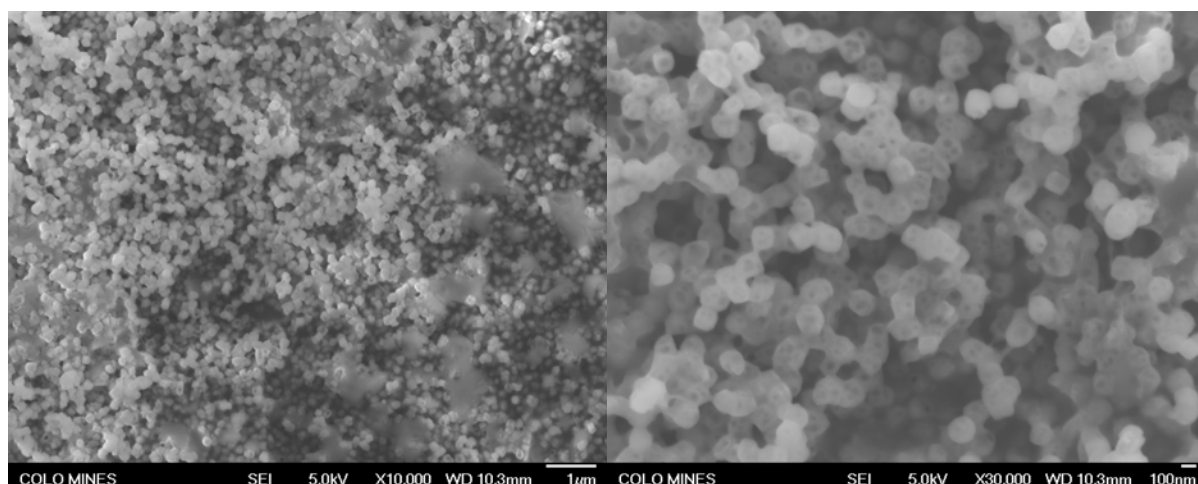


**Figure 5:** SEM images of  $\text{Na}_2\text{S}$  crystals produced by reacting sodiummethoxide in DME with  $\text{H}_2\text{S}$

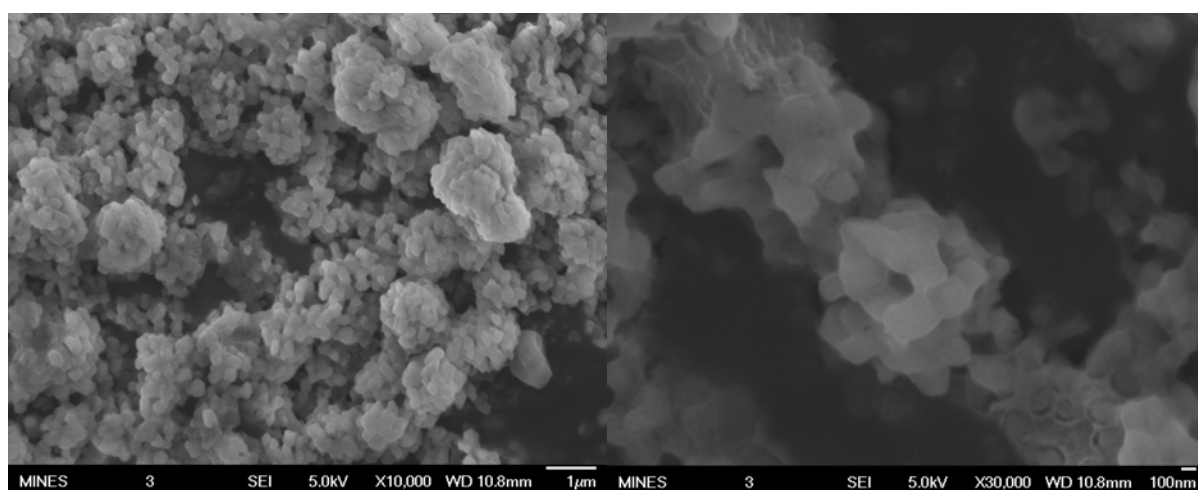


**Figure 6:** SEM images of  $\text{Na}_2\text{S}$  crystals produced by reacting sodiumbutoxide in DME with  $\text{H}_2\text{S}$

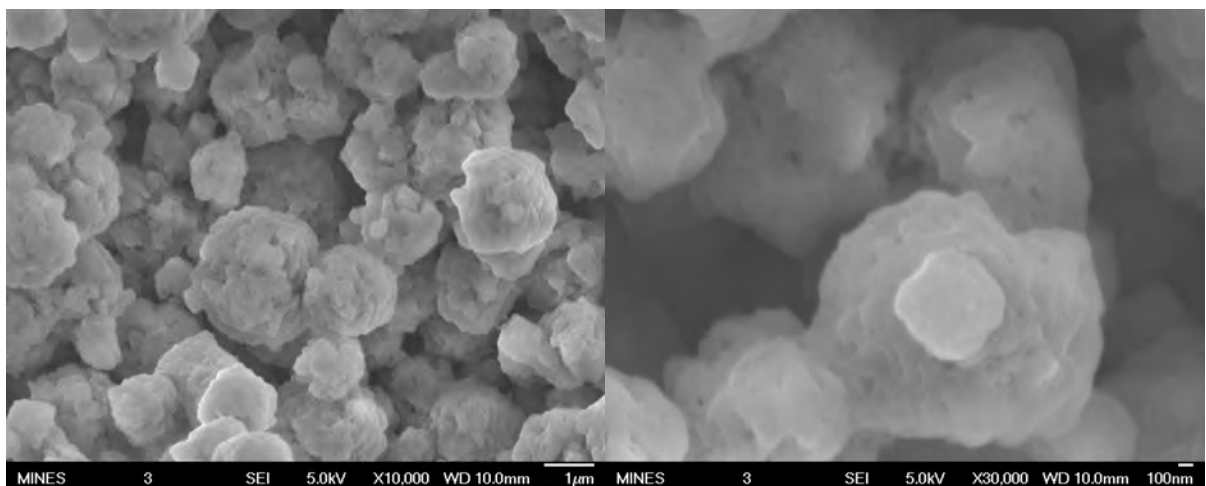


**Figure 7:** SEM images of Na<sub>2</sub>S crystals produced by reacting sodiummethoxide in MeTHF with H<sub>2</sub>S

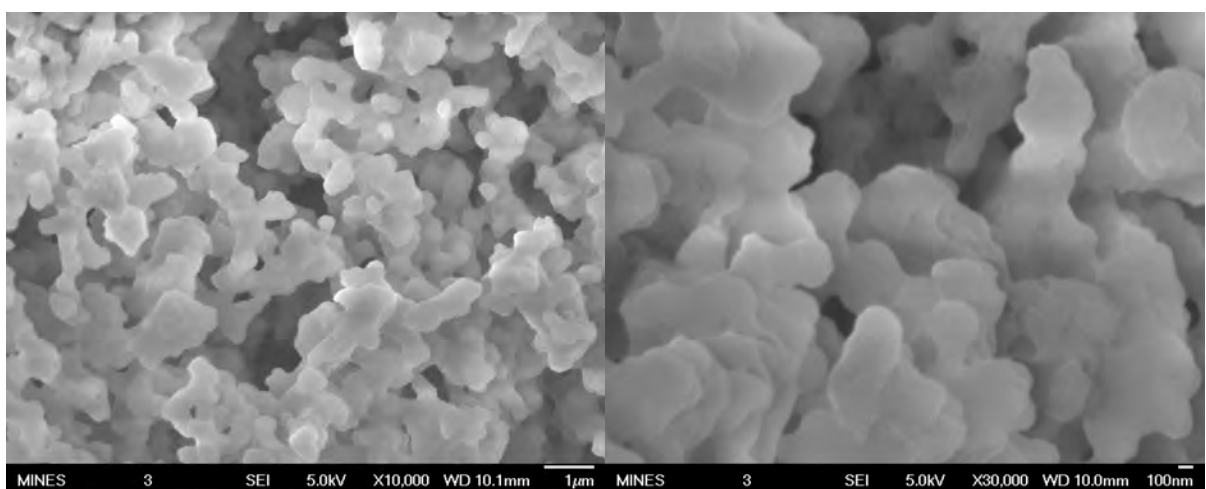


**Figure 8:** SEM images of Na<sub>2</sub>S crystals produced by reacting sodiumbutoxide in MeTHF with H<sub>2</sub>S

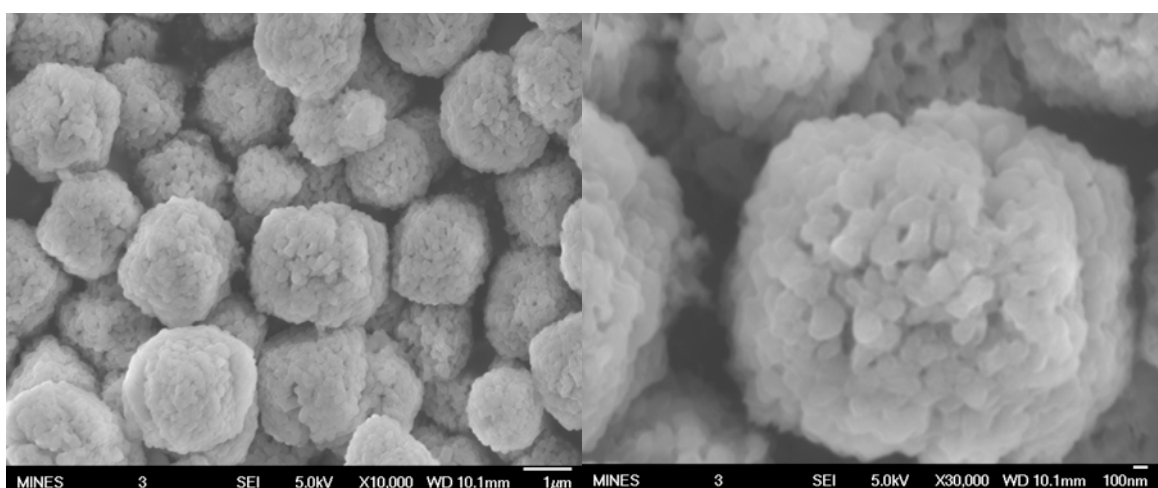


**Figure 9:** SEM images of Na<sub>2</sub>S crystals produced by reacting sodiummethoxide in dioxane with H<sub>2</sub>S



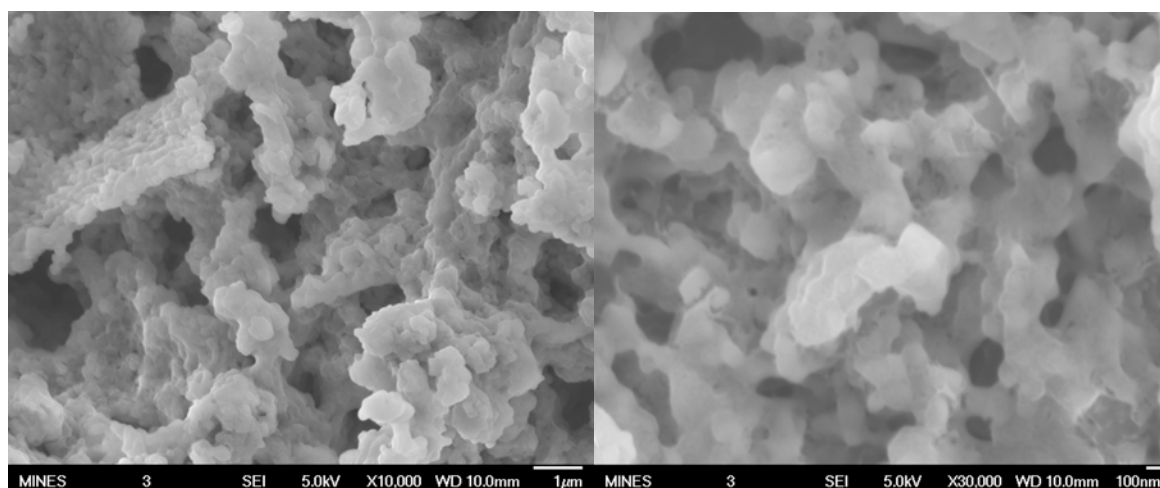


**Figure 10:** SEM images of Na<sub>2</sub>S crystals produced by reacting sodiumbutoxide in dioxane with H<sub>2</sub>S

### Discussion and Conclusions:

From this research we can conclude that longer carbon chain alcohols (hexanol & octanol) are not compatible with this method of Na<sub>2</sub>S production. These results were puzzling at first as we thought that fact that these longer carbon chain alcohols are stronger bases would facilitate the desired reaction. However, upon further consideration, we hypothesise that the complete dissociation of H<sub>2</sub>S to S<sup>2-</sup> requires a more strongly polar environment than that provided by hexanol and octanol.

It was also very surprising to us that systems in which DBE was used as a solvent did not produce pure Na<sub>2</sub>S. However, a similar argument can be made for DBE, as was made for hexanol and octanol above. Of all the solvents investigated, DBE is the least polar. It only has a single oxygen atom, is highly symmetrical and has relatively long carbon chains on either side of the oxygen atom. This may have inhibited the required dissociation of H<sub>2</sub>S to S<sup>2-</sup>.

An alternative hypothesis is also being considered. This is prompted by concurrent research which has shown that when lithium is used instead of sodium, pure Li<sub>2</sub>S can only be produced when the DBE is added to the lithium ethanol solution immediately prior to commencement of the reaction with H<sub>2</sub>S. This indicates that lithium may react with DBE with a relatively slow reaction rate. The valence electron of sodium is further away from the nucleus than that of lithium. Thus, the attraction between the nucleus and the outer electron is weaker, meaning that it is more easily lost. Based on these facts, we are considering whether the sodium reacts with the DBE with a greater reaction rate, thus inhibiting the desired reaction between the sodium and the H<sub>2</sub>S.

All of the other solvents investigated, (DME, MeTHF and Dioxane) successfully yielded pure Na<sub>2</sub>S crystals.

However, the morphologies of these crystals varied widely both as the alcohol and the solvent changed. The next step in this process will be to assemble cathodes from the Na<sub>2</sub>S crystals of different morphologies. This will allow the determination of the structure-property-performance relationship.

Prior to conducting the aforementioned experiments, we would hypothesise that the secondary structures formed in all of the systems apart from the ethanol in DME will result in batteries with superior energy density. This is because they will facilitate greater packing densities of the nanoparticles. However, this superior energy density is dependent on being able to incorporate a carbon scaffold within the secondary structures. As Na<sub>2</sub>S is a poor ionic and electrical conductor, there would be poor active material utilisation if the carbon scaffold merely went around the secondary structures rather than intersect them. This will be of particular importance if the sodiummethoxide in MeTHF or the sodiummethoxide in dioxane systems are used. These systems result in the formation of relatively large, spherical secondary structures with a small surface area to volume ratio. Without a carbon scaffold within these spheres there would be a lot of Na<sub>2</sub>S that would not participate in the battery cycling.

It is hypothesized that solubility is a major factor in determining the morphology of the synthesised Na<sub>2</sub>S crystals. It is known that chemicals with higher solubility typically precipitate in smaller sizes, (Peng *et al.*, 1998). Further experimentation is required to quantify the solubility of Na<sub>2</sub>S in each of the systems investigated in this study and to investigate if these results correlate with the observed particle sizes. However, it is already known that Na<sub>2</sub>S is more soluble in ethanol than it is in butanol. The alcohol was always present in excess in our reactions. Therefore, this suggests that when the same solvent

is used the nanocrystals synthesised using ethanol should be smaller than the nanocrystals synthesised using butanol. In our study it appears as though the ethanol systems did tend to produce slightly smaller nanoparticles. However, there is a need to conduct further experiments to confirm these preliminary findings.

Aside from particle size, the morphologies vary dramatically between the ethanol and butanol systems. They form very different secondary structures, (individual small particles, relatively large spherical clusters or coral-like arrangements) and some of the nano crystals are cubic whereas others are more plate-like. This suggests that factors other than solubility influence the morphology and aggregation of Na<sub>2</sub>S nanocrystals synthesised in this manner, and perhaps even, that these factors dominate over the influence of solubility.

The degree to which the growth of the nanocrystals is diffusion limited in the various systems could play a major role. Furthermore, it has been suggested that nucleation takes place rapidly at high concentrations, (Peng *et al.*, 1998). This suggests that if the flow rate of H<sub>2</sub>S was increased, thus increasing the concentration of Na<sub>2</sub>S in the solution, nucleation may occur in preference to growth, which would result in more numerous, smaller nanocrystals. Finally, the Gibbs- Thomson equation, (figure 11) includes temperature as a determining factor in the growth of the nanocrystals.

For commercial applications, the yield of Na<sub>2</sub>S will be important. Apart from the reactions that took place in DME, it appears as though a higher yield can be achieved when sodium butoxide is reacted with H<sub>2</sub>S rather than when sodium ethoxide is reacted with H<sub>2</sub>S. This is logical as Na<sub>2</sub>S is more soluble in ethanol than in butanol. The deviation from this for the DME system could be explained by the fact that a different researcher carried out the ethanol elements of the DME experiment.

$$S_r = S_b \exp(2\sigma V_m / rRT)$$

$S_r$  = Solubility of nanocrystal  
 $S_b$  = Solubility of bulk solid  
 $\sigma$  = Specific surface energy  
 $r$  = Radius of nanocrystal

Figure 11: Gibbs- Thomson equation

#### References:

- Adelhelm P., Hartmann P., Bender C.L., Busche M., Eufinger C., Janek J., (2015). "From lithium to sodium: cell chemistry of room temperature sodium- air and sodium- sulfur batteries". *Beilstein J. Nanotechnol.* 6: 1016- 1055
- Li X., Morrish R.M., Yang Y., Wolden C.A., Yang Y., (2015). "Thermodynamically Favorable Conversion of Hydrogen Sulfide into Valuable Products through Reaction with Sodium Naphthalenide". *ChemPlusChem* 80: 1508-1512
- Peng X.G., Wickham J., Alivisatos A.P., (1998). *Kinetics of II-VI and III-V colloidal semiconductor nanocrystal growth: "Focusing" of size distributions*, *Journal of the American Chemical Society* 120: 5343-5344.
- Sudworth J.L. & Tilley A.R., (1985). "The Sodium Sulfur Battery" Chapter 2 Chapman & Hall.
- Wei S., Xu S., Agrawal A., Choudhury S., Lu Y., Tu Z., Ma L., Archer L.A., (2016). "A stable room-temperature sodium- sulfur battery". *Nature Communications* 7: 11722.
- Wu F., Kim H., Magasinski A., Lee J.T., Lin H.T., Yushin G., (2014). "Harnessing Steric Separation of Freshly Nucleated Li<sub>2</sub>S nanoparticles for Bottom- Up Assembly of High Performance Cathodes for Lithium-Sulfur and Lithium- Ion Batteries". *Adv. Energy Mater* 4: 1400196.

## Appendix 1: Comparison of results using dioxane before and after treatment with sodium

### Motivation:

Sodiummethoxide in dioxane was reacted with  $H_2S$  twice. The first time, dioxane was used directly from the bottle.  $Na_2S$  was formed but some sulfide absorbed water and formed hydrates. It was proposed that the dioxane may not be completely anhydrous. To remedy this, the dioxane was pretreated with sodium so that any water present would react with the sodium. The reaction with  $H_2S$  was then repeated with this pretreated sodium.

### Morphology:

The first  $Na_2S$  sample, in which hydrates were detected, exhibits a pretty uniform morphology. Cubes with an edge length in the region of  $1\mu m$  are formed. It is difficult to distinguish the individual nanocrystals from which these microstructures are formed, (figure 12). In contrast, two distinct  $Na_2S$  morphologies were identified in the sample from the second reaction (figure 13). Figure 13a shows a cube composed of many nanoparticles with edge lengths of approximately 100nm. The morphology shown in figure 13b is very similar to that obtained from the first reaction in which hydrates were detected. These findings can be explained further by looking at the two samples under less magnification. At X1,000 magnification we can see that the cubes formed in the first reaction are all connected to each other, (figure 14a). However, in the sample from the second reaction, there appears to be regions in which the cubes are connected to each other and other regions in which they appear to exist independently, (figure 14b). We hypothesise that the morphology shown in figure 13a exists in the region where all of the cubes exist independently and that the morphology shown in figure 13b exists in the region where all of the cubes are connected to each other.

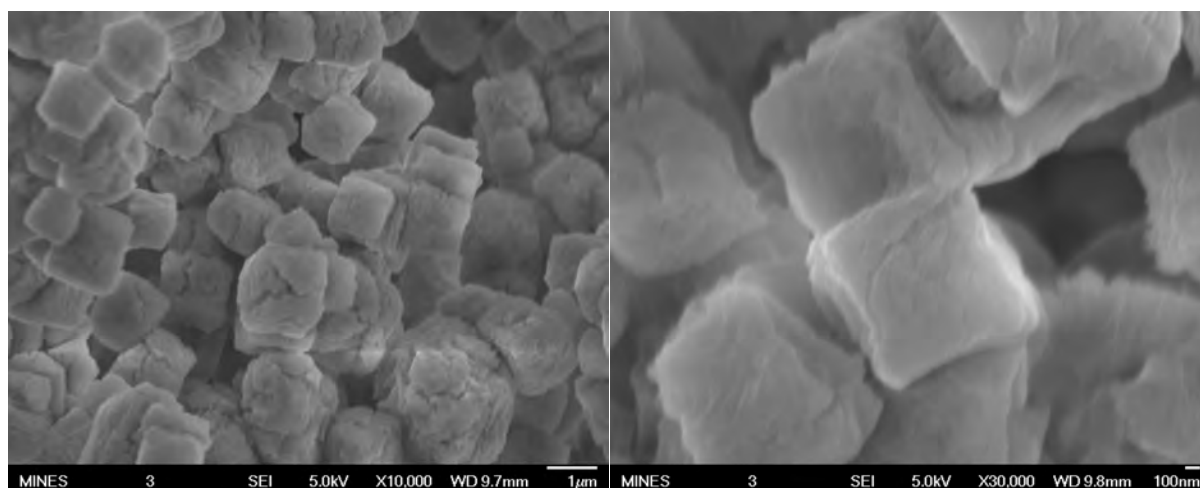


Figure 12: SEM images at different magnification from the first reaction of sodiummethoxide in dioxane with  $H_2S$

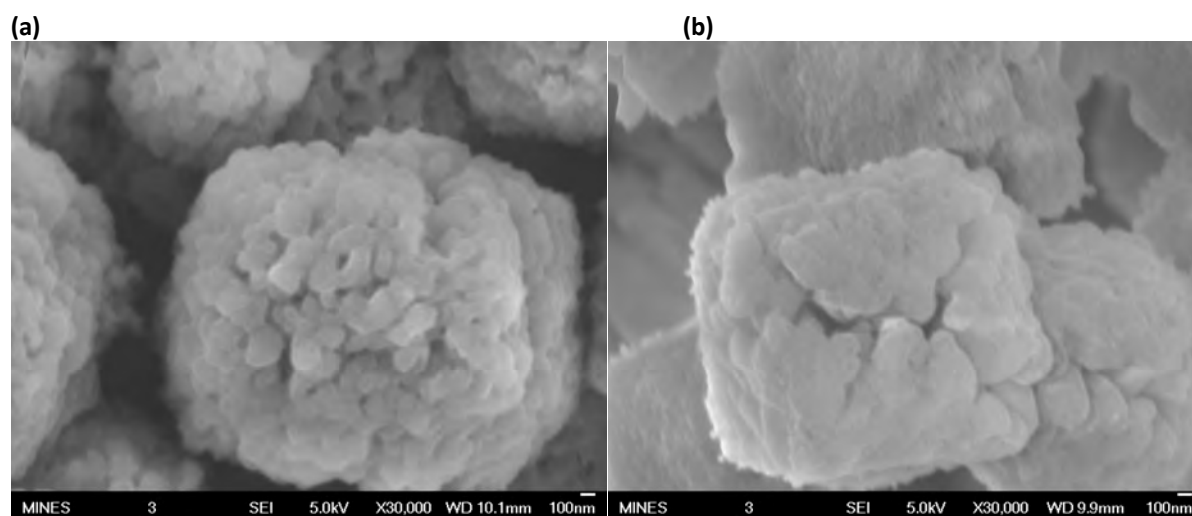
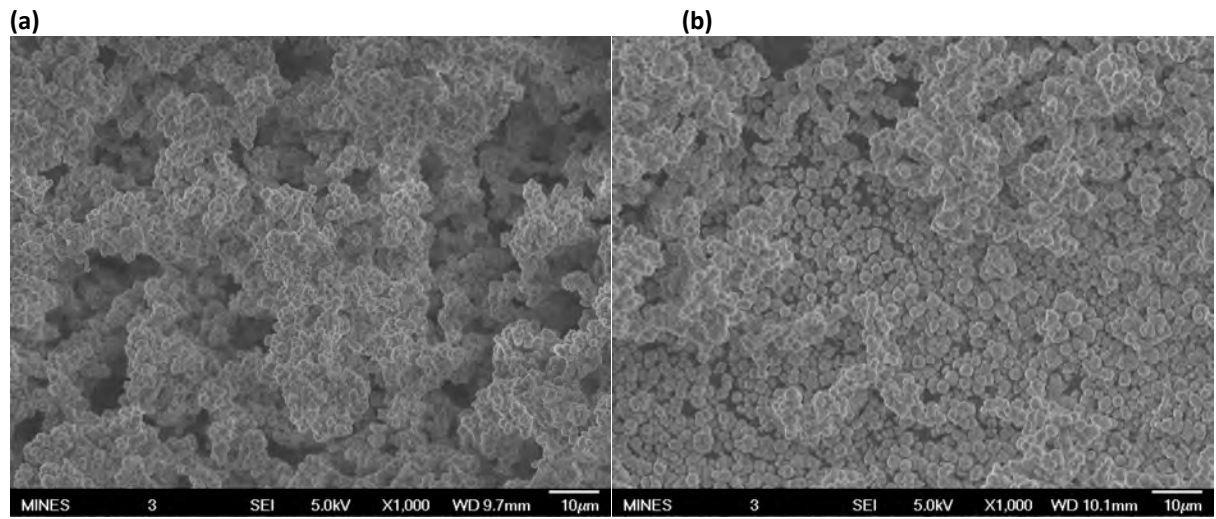


Figure 13: SEM images showing the different morphologies yielded in the second reaction of sodiummethoxide in dioxane with  $H_2S$



**Figure 14:** SEM images showing a) the uniform morphology yielded from the first reaction and b) the two distinct morphologies